State transitions in *Chlamydomonas reinhardtii* strongly modulate the functional size of photosystem II but not of photosystem I

Caner Ünlü[a], Bartlomiej Drop[b], Roberta Croce[b], and Herbert van Amerongen[a,c,1]

[a]Laboratory of Biophysics and [c]MicroSpectroscopy Centre, Wageningen University, 6703 HA, Wageningen, The Netherlands; and [b]Department of Physics and Astronomy, Faculty of Sciences, VU University Amsterdam, 1081 HV, Amsterdam, The Netherlands

Edited* by Graham R. Fleming, University of California, Berkeley, CA, and approved January 29, 2014 (received for review October 18, 2013)

Plants and green algae optimize photosynthesis in changing light conditions by balancing the amount of light absorbed by photosystems I and II. These photosystems work in series to extract electrons from water and reduce NADP$^+$ to NADPH. Light-harvesting complexes (LHCs) are held responsible for maintaining the balance by moving from one photosystem to the other in a process called state transitions. In the green alga *Chlamydomonas reinhardtii*, a photosynthetic model organism, state transitions are thought to involve 80% of the LHCs. Here, we demonstrate with picosecond-fluorescence spectroscopy on *C. reinhardtii* cells that, although LHCs indeed detach from photosystem II in state 2 conditions, only a fraction attaches to photosystem I. The detached antenna complexes become protected against photodamage via shortening of the excited-state lifetime. It is discussed how the transition from state 1 to state 2 can protect *C. reinhardtii* in high-light conditions and how this differs from the situation in plants.

time-resolved fluorescence spectroscopy | photoprotection

Oxygenic photosynthesis is the most important process for fueling life on earth. Light capture and subsequent charge separation processes occur in the so-called photosystems I and II (PSI and PSII). In plants and green algae, both PSs consist of a pigment–protein core complex surrounded by outer light-harvesting complexes (LHCs). Electronic excitations induced by the absorption of sunlight lead to charge separation in the reaction centers (RCs) of PSI and PSII, located in the cores of the PSs. These PSs work in series to extract electrons from water and reduce NADP$^+$ to NADPH. For optimal linear electron transport from water to NADP$^+$, a balance is needed for the amount of light absorbed by the pigments in the two PSs.

Besides carotenoids, the PSII core contains 35 chlorophylls *a* (Chls *a*), whereas this number is close to 100 for PSI (1). The outer LHCs consist of various components: The major light-harvesting complex LHCII (a trimer) harbors 12 carotenoids (Cars) and 42 chlorophylls (Chls), 24 of which are Chls *a* (2), the pigments that are largely responsible for excitation energy transfer (EET) to the PSII RC. In higher plants, there are also three monomeric minor LHCs per core, called CP24, CP26, and CP29, which show high sequence homology with LHCII (see, e.g., ref. 3). In nonstressed conditions, between 85% and 90% of the excitations in PSII lead to charge separation in the RC (4). PSI in plants binds four LHCs (Lhca1–4) (5). The amount of LHCII in the plant membranes is variable and usually ranges from approximately two to approximately four trimers per PSII core, most of which are functionally connected to PSII, although part is also associated with PSI (6). In *Chlamydomonas reinhardtii*, PSI antenna size differs and there are nine Lhcas per PSI (7). Nine LhcbM genes, plus CP29 and CP26, codify for the antenna complexes of PSII (8), and it was recently shown that, in addition to CP26 and CP29, the PSII supercomplex contains three LHCII trimers per monomeric core (9). In addition, there are usually three to four extra LHCII trimers present per monomeric core (10) (see also below).

Although both PSI and PSII contain Chls and Cars, their absorption spectra differ, with PSII being more effective in absorbing blue light and PSI in absorbing far-red light (11–13). Because intensity and spectral composition can vary, organisms need to rapidly adjust the relative absorption cross-sections of both PSs. This regulation occurs via so-called state transitions, and it involves the relocation of Lhcs between PSII and PSI (14).

In higher plants, all LHCII is bound to PSII in state 1, whereas in state 2, which can be induced by overexciting PSII, part of LHCII (around 15%) moves to PSI (14, 15). State transitions are regulated by the state of the plastoquinone (PQ) pool via the reversible phosphorylation of LHCII (14, 16–19). The green alga *C. reinhardtii*, which has widely been used as a model system in photosynthesis research and which might also become important for the production of food and feed ingredients and future biofuels (20), is thought to exhibit state transitions to a far larger extent than higher plants. The widely accepted view is that, during the transition from state 1 to state 2, 80% of the major antenna complexes dissociates from PSII and attaches to PSI (21). This picture is based on results that were obtained with photoacoustic measurements that were used to determine the quantum yield of both PSs in different states. This view has been supported by the finding that the PSII supercomplex is largely disassembled in state 2 (22). However, although a PSI–LHCII supercomplex from *C. reinhardtii* has been isolated (23), the amount of LHCII associated with it has not been quantified and it has also not been shown that the additional LHCII is capable

Significance

To optimize their photosynthetic performance, most oxygen-evolving organisms are able to shuttle light-harvesting pigment–protein complexes between photosystems I and II. These photosystems work in series to transform light energy into chemical energy. It is generally accepted that 80% of the light-harvesting complexes is participating in the reorganization in the green alga *Chlamydomonas reinhardtii*, a model organism for photosynthesis research. However, in the present paper, we demonstrate that such a large remodeling does not occur. Light-harvesting complexes can indeed detach from photosystem II, but only a small fraction subsequently attaches to photosystem I, and it is demonstrated how this leads to photoprotection in high-light conditions. This phenomenon has significant implications for our way of thinking about the efficiency regulation in photosynthesis.

Author contributions: C.Ü., R.C., and H.v.A. designed research; C.Ü. and B.D. performed research; C.Ü., B.D., R.C., and H.v.A. analyzed data; and C.Ü., R.C., and H.v.A. wrote the paper.

The authors declare no conflict of interest.

*This Direct Submission article had a prearranged editor.

[1]To whom correspondence should be addressed. E-mail: herbert.vanamerongen@wur.nl.

This article contains supporting information online at www.pnas.org/lookup/suppl/doi:10.1073/pnas.1319164111/-/DCSupplemental.

of transferring energy to the PSI core. More recently, it was argued based on biochemical analysis that also CP26 and CP29 are participating in state transitions in *C. reinhardtii* (22–25), but again a quantitative analysis is missing.

Besides biochemical techniques, time-resolved fluorescence spectroscopy can be helpful to study state transitions and to enlighten the EET processes. The main advantage of this technique is that it can provide both quantitative and functional information for the different states in vivo (6). However, the number of time-resolved fluorescence studies on green algae and especially their state transitions is limited (26–29). Wendler and Holzwarth (27) studied state transitions in the green alga *Scenedesmus obliquus* using time-resolved fluorescence spectroscopy. They interpreted their data at that time in terms of reversible migration of LHCs between PSII α- and β-centers during state transitions, whereas it was concluded that the size of PSI was not measurably changing (27). Another study was performed by Iwai et al. (28), who used fluorescence lifetime imaging microscopy (FLIM) to visualize state transitions in *C. reinhardtii*. The authors reported the dissociation of LHCII from PSII during the first part of the transition from state 1 to state 2, but they did not investigate what was happening during the later phase (28). Recently, Wientjes et al. (6) performed a study on light acclimation and state transitions in the plant *Arabidopsis thaliana*, and among others it was demonstrated quantitatively how time-resolved fluorescence properties of thylakoid membranes change when the relative amount of LHCII attached to PSI and PSII changes (6): When LHCII attaches to PSI, the amplitude of a component with fluorescence lifetime below 100 ps increases significantly, whereas the contribution of the components with lifetimes of several hundreds of picoseconds concomitantly decreases, and the corresponding lifetimes become shorter (6). The former component is mainly due to PSI (with or without LHCII connected) and the latter are due to PSII (with varying amounts of LHCII connected). It is important to point out that the amplitudes of the decay components are directly proportional to the number of pigments that correspond to these decay components (6, 30). Therefore, if during state transitions LHCs are moving from PSII to PSI, then the amplitude(s) of the PSI decay components will increase, whereas those of PSII will decrease. In general, such a reorganization will also lead to some changes in the fluorescence lifetimes. If in addition also quenching processes are introduced, this will lead to an additional change in the lifetime but not in the amplitude (31).

Here, we applied time-resolved fluorescence spectroscopy to study changes in PSI and PSII antenna size in response to state transitions for wild-type (WT) *C. reinhardtii* in vivo. The cells were locked in different states, using the same method as used for previous photoacoustic measurements (21, 32), and fluorescence decay curves were recorded at room temperature. The results lead us to challenge some of the generally accepted views, especially concerning the structure of the PSI supercomplex in state 2 and the fate of the detached LHCII. The main changes during state transitions occur in PSII, whereas changes in the PSI supercomplex turn out to be less pronounced. In addition, it appears that both in state 1 and 2 a pool of LHCII exists that is neither connected to PSI nor to PSII, whereas its size is larger in state 2.

Results

Low-Temperature Steady-State Fluorescence. The 77 K steady-state fluorescence spectra of state 1- and state 2-locked cells of WT *C. reinhardtii* were recorded upon 440-nm excitation (Fig. 1). The spectra show the changing ratio of the intensity at 688 and 710 nm, which is characteristic for state transitions. The difference in ratio is thought to indicate that more LHCs are associated with PSII (fluorescence around 688 nm) in state 1 than in state 2 when LHCs largely associate with PSI (fluorescence around 710 nm). To study the underlying processes in more detail, we performed time-resolved fluorescence measurements in vivo at room temperature.

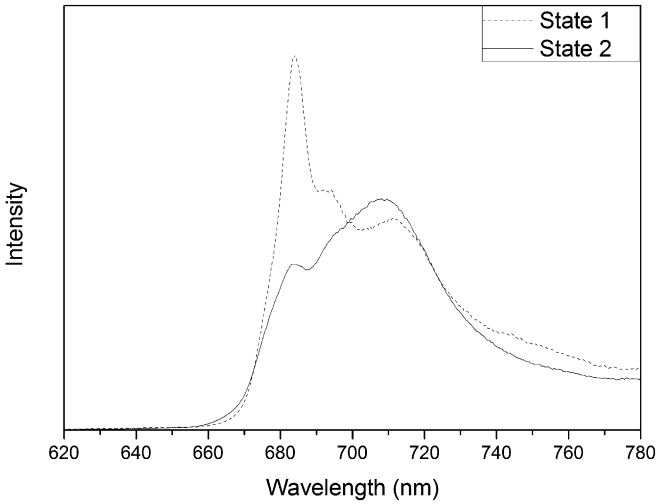

Fig. 1. The 77 K fluorescence spectra of state 1-locked (dash) and state 2-locked (line) *C. reinhardtii* cells. The λ_{exc} was 440 nm. Note that the concentrations of the cells were identical for both states, and the same was true for all of the settings of the fluorimeter. Therefore, the intensities of the spectra can be directly compared with each other in an absolute sense. The fluorescence quantum yield of PSI in state 2 is only slightly higher than in state 1.

Room Temperature Time-Resolved Fluorescence. Time-resolved fluorescence measurements of *C. reinhardtii* cells in state 1 and 2 were performed with a time-correlated single photon counting (TCSPC) setup. Subpicosecond laser pulses of 400 nm, exciting relatively more Chls *a*, and pulses of 465 nm, exciting relatively more Chls *b* (and thus more antenna complexes) were used (33, 34). For detection, use was made of 679-, 701-, and 720-nm interference band filters. Fig. 2 shows that the fluorescence decay kinetics of state 1-locked cells is somewhat slower than those of cells in state 2 for every excitation (λ_{exc}) and detection wavelength (λ_{det}) and the exact difference depends on the combination of wavelengths.

To obtain quantitative information from these decay curves, global analysis was performed and for all excitation and detection wavelengths the curves were fitted with the same lifetimes, at least for a specific state (6), even though individual lifetimes do not necessarily correspond one-to-one to specific physical processes. Global analysis of fluorescence decay curves of state-locked *C. reinhardtii* cells requires five decay components but the very fast one (~1 ps) has no real physical meaning because it is far shorter than the instrument response function (IRF), and it does not have to be considered further (*Methods*). The residual plots for all different state-locked cells in *SI Text* (Fig. S1) demonstrate that five exponentials are sufficient. Fitting results are given in Tables 1 and 2.

The lifetime τ_1 in Tables 1 and 2, which is in the range 65–75 ps, is mainly due to PSI (27, 30). Because PSI fluorescence is red-shifted compared with PSII fluorescence, the relative amplitude of this component increases upon going from 679 nm to 720 nm. Only small changes occur in both the value of τ_1 and the corresponding amplitude due to the state change in *C. reinhardtii*. For λ_{exc} = 400 nm, τ_1 is identical for state 1 and 2, and the corresponding amplitude is also the same. For λ_{exc} = 465 nm, τ_1 is 6 ps shorter for state 1 than for state 2, whereas the corresponding amplitude is ~4% higher in state 2. Therefore, although some increase of both amplitude and lifetime of the PSI component can be observed, this increase is far smaller than one

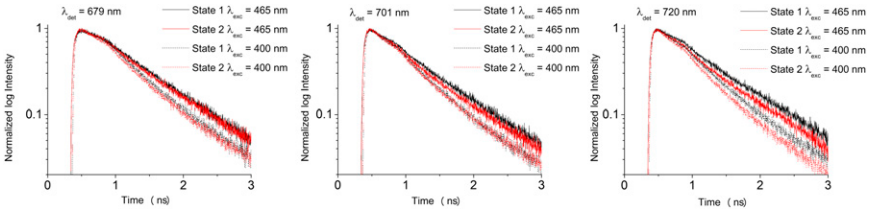

Fig. 2. Fluorescence decay curves for state 1- (black) and state 2-locked (red) *C. reinhardtii* cells at λ_{det} of 679, 701, and 720 nm and excited at 465 and 400 nm. These data were globally analyzed by TRFA software.

might expect based on literature (21). The small increase in lifetime and amplitude lead to a small increase of the amount of PSI steady-state fluorescence, which becomes more pronounced at 77 K and is (largely) responsible for the change in the ratio of fluorescence at 688 and 720 nm (Fig. 1).

The lifetimes τ_2 and τ_3 in Tables 1 and 2 are mainly due to PSII with the highest amplitude at $\lambda_{det} = 679$ nm, as expected for PSII (27); there is also some contribution from disconnected LHCs (discussed below). Lifetime τ_2 becomes shorter in state 2, 216 ps instead of 266 ps for $\lambda_{exc} = 400$ nm, but for $\lambda_{exc} = 465$ nm, τ_2 remains more or less unchanged, 259 ps for state 2 vs. 254 ps for state 1. The amplitude remains the same for both excitation wavelengths. The shortening of τ_3 upon going to state 2 is more pronounced: for $\lambda_{exc} = 400$ nm, τ_3 goes down from 663 to 551 ps, whereas the amplitude remains more or less constant, and for $\lambda_{exc} = 465$ nm from 837 to 715 ps, whereas the amplitude drops by 12%. In general, the average lifetime for PSII is shorter in state 2 (for both excitation wavelengths), whereas the total amplitude remains more or less constant for $\lambda_{exc} = 400$ nm. Finally, the small contribution (at most 3%) of the longest component (τ_4) in state 1-locked cells is ascribed to some free chl but mainly to disconnected LHCs [note that the contribution of τ_4 to the average lifetime was even smaller when cells were grown in higher light conditions (*SI Text*, Table S1)]. However, it should be noted that the amplitude of τ_4 increases for state 2-locked cells (5% at $\lambda_{exc} = 400$ nm, 10% at $\lambda_{exc} = 465$ nm when detecting at 679 nm), which may be due to an increase of the amount of disconnected LHCs (26).

The main purpose of the present study is to understand the functional/organizational differences for PSI, PSII, and dissociated LHCII in state 1 and 2. Whereas PSI has its own characteristic red-shifted fluorescence, the spectra of PSII and LHCII at room temperature largely overlap. To at least qualitatively distinguish between PSII and LHCII, the fluorescence decay kinetics was measured for state 1- and state 2-locked cells using different excitation wavelengths: 400 nm (excites relatively more the PSII core complexes) and 465 nm (excites relatively more the outer antenna complexes) (34). Comparison of the decay curves for both excitation wavelengths shows that the decay is significantly slower for $\lambda_{exc} = 465$ nm, both in state 1 and 2. Whereas τ_1 predominantly reflects the PSI decay time τ_2–τ_4 correspond to PSII and LHCII, and because it is a priori difficult to discriminate between PSII and LHCII, we start by considering these lifetimes together. For state 1, the amplitude-weighted average lifetime τ_{avg} of τ_2–τ_4 is 547 ps for $\lambda_{exc} = 400$ nm (relatively more core excitation), whereas it is 660 ps for $\lambda_{exc} = 465$ nm ($\lambda_{det} = 679$ nm in both cases). The substantial difference (113 ps) indicates that either part of the antenna complexes is very badly connected to PSII core or not connected at all (30). The same conclusion can be drawn from the data on state 2-locked cells, where τ_{avg} is 510 ps for $\lambda_{exc} = 400$ nm, and it is 638 ps for $\lambda_{exc} = 465$ nm ($\lambda_{det} = 679$ nm in both cases). In conclusion, both for state 1- and state 2-locked cells, we find a substantial fraction of badly connected or even fully detached LHCII. To confirm that this is an intrinsic property of individual cells and it is not due to a fraction of damaged or dead cells, we also performed two-photon FLIM experiments to monitor the variation between cells and a typical picture with densely packed cells is given in Fig. 3, demonstrating that the fluorescence lifetime of all cells are very similar (on average around 400 ps) and thus that these long lifetime components are indeed an intrinsic property of individual *C. reinhardtii* cells. It is worth mentioning that the FLIM lifetimes that were previously determined by Minagawa and coworkers (28) were far shorter (around 200 ps), possibly because of the high excitation densities in their one-photon FLIM experiments, which can lead to singlet–singlet annihilation (35). In contrast, it is possible with the two-photon FLIM setup used here to record images with lifetimes that are very similar to lifetimes that are obtained with "macroscopic" TCSPC and streak-camera picosecond fluorescence setups (36, 37).

Discussion

Energy partitioning between PSI and PSII has already been the subject of intense research for many years (13, 38). Genetics approaches have led to the discovery of key proteins involved, such as kinases and phosphatases, regulating the phosphorylation state of LHCII and its relocation between PSII and PSI (16, 19, 39). Biochemical and physiological studies have provided information about the mechanism and importance of state transitions in plants (40, 41) and the green alga *C. reinhardtii* (22, 23). Important differences seem to exist between state transitions in *C. reinhardtii* and plants, such as the participation of the monomeric antennae CP26 and CP29 only in *C. reinhardtii* (22, 23) and the percentage of LHCII that participates (80% for *C. reinhardtii* vs. 15% for higher plants) (14, 21).

Recently, long-term acclimation and state transitions in *A. thaliana* were studied in detail, using amongst others time-resolved fluorescence techniques (6). It was shown that the amplitude of the fluorescence lifetime that is due to PSI increases significantly when LHCII becomes attached to it (21). It is thus remarkable that in *C. reinhardtii* only relatively minor differences can be observed between the PSI fluorescence kinetics for states

Table 1. Global analysis results for TCSPC data obtained by excitation at 400 nm at room temperature for state-locked *C. reinhardtii*

		λ_{det}, nm		
		679	701	720
State	τ, ps	*p*	*p*	*p*
State 1				
	67 (τ_1)	0.36	0.55	0.56
	266 (τ_2)	0.28	0.23	0.20
	663 (τ_3)	0.33	0.21	0.23
	1,902 (τ_4)	0.03	0.01	0.01
State 2				
	66 (τ_1)	0.38	0.54	0.55
	216 (τ_2)	0.25	0.21	0.20
	551 (τ_3)	0.29	0.22	0.22
	1,285 (τ_4)	0.08	0.03	0.03

Confidence intervals of fluorescence lifetimes (τ) as calculated by exhaustive search were <5%; lifetimes were calculated from two to four repeats; *p* indicates relative amplitudes.

Table 2. Global analysis results for TCSPC data obtained by excitation at 465 nm at room temperature for state-locked *C. reinhardtii*

		λ_{det}, nm		
		679	701	720
State	τ, ps	*p*	*p*	*p*
State 1				
	68 (τ_1)	0.39	0.54	0.54
	254 (τ_2)	0.24	0.20	0.19
	837 (τ_3)	0.34	0.23	0.24
	1,909 (τ_4)	0.03	0.03	0.03
State 2				
	74 (τ_1)	0.43	0.58	0.57
	259 (τ_2)	0.24	0.20	0.20
	715 (τ_3)	0.20	0.15	0.14
	1,222 (τ_4)	0.13	0.08	0.09

Confidence intervals of fluorescence lifetimes (τ) as calculated by exhaustive search were <5%; lifetimes were calculated from two to four repeats; *p* indicates relative amplitudes.

1 and 2, whereas the percentage of moving antenna is thought to be much higher (80% vs. 15%). If indeed 80% of the LHCII would move from PSII to PSI upon going from state 1 to state 2, this should lead to an increase of the relative amplitude of the PSI component by almost 40% (*SI Text*), but the observed increase is at most 4%. Even if on average only one LHCII trimer would move from PSII to PSI this should still already lead to an increase of PSI amplitude by 6% (*SI Text*). Therefore, it should be concluded that the change in the average size of PSI is clearly smaller than one might have expected. This is further supported by the fact that also the corresponding lifetime hardly increases (only by 6 ps, at most).

To confirm in an independent way the fact that the amount of LHCII moving to PSI is substantially lower than what is generally believed, we also recorded 77 K fluorescence excitation spectra in states 1 and 2, while monitoring the fluorescence of PSI at 712 nm and of PSII/LHCII at 680 nm (*SI Text*, Fig. S2). When comparing the excitation spectra of PSI and PSII, it is clear that the spectral contributions around 475 and 650 nm are much smaller for PSI. These contributions are arising from Chl *b* and thus from the connected LHCs. Upon going from state 1 to state 2, there is a minor increase of this contribution for PSI (in particular around 650 nm), whereas a small decrease can be observed for PSII (especially around 475 nm). So the low-temperature fluorescence excitation spectra confirm the fact that little LHC is moving to PSI. A similar conclusion can be drawn from the 77 K emission spectra recorded for different excitation wavelengths (*SI Text*, Fig. S3).

Although the changes in amplitude and lifetime of PSI are relatively minor, there is, however, a significant decrease of the average lifetime (not amplitude) of the slower decay components, which are usually thought to originate from PSII. Our data imply that there must be a substantial change in PSII organization in agreement with earlier biochemical data (22). The decrease of the average "PSII" lifetime can in principle be explained by a mechanism that is partly similar to the one that was recently proposed by Minagawa and coworkers (28). According to this mechanism, a dynamic equilibrium exists between LHCII associated to PSII, LHCII associated to PSI, and LHCII dissociated from both PSs, being self-aggregated in a separate LHCII pool, where the fluorescence (excited state) of LHCII is quenched. In state 1, the majority of LHCII is bound to PSII, whereas for state 2 the equilibrium shifts direction LHCII bound to PSI via aggregated LHCII. Our data do not confirm the association of a large amount of LHCII to PSI (at most a small fraction of LHCII becomes associated to PSI), but the fact that the "PSII lifetimes" become faster in state 2 while the total amplitude remains similar, can be explained by the detachment of LHCII from PSII while at the same time LHCII becomes quenched; otherwise one would expect the appearance of long-lived fluorescence component of around 4 ns (42). A simple explanation for such quenching can indeed be aggregation of LHCII: Compared with monomeric and trimeric LHCII, aggregated LHCII is heavily quenched and the corresponding lifetimes can even be as short as 30 ps, although a typical average lifetime is several hundreds of picoseconds (42). For a complete understanding of the phenomenon of state transitions, it is important to sort out whether LHCII really dissociates and aggregates upon going from state 1 to state 2, and to do so we compared the kinetics for excitation at different wavelengths.

In a previous picosecond fluorescence study on thylakoid membranes from *A. thaliana*, van Oort et al. (30) used two excitation wavelengths to maximally vary the relative number of excitations in the core and outer antenna of PSII. The main purpose of that work was to determine the migration time of excitations to the RCs and to separate the PSI and PSII fluorescence kinetics from each other. It was, however, also found that in a CP24-less mutant, part of the outer antenna is detached from the PSII core, leading to a substantial increase of the fluorescence lifetime when relatively more outer antenna is excited. At the same time, it could be concluded that this detached antenna was quenched because the fraction of pigments with a long fluorescence lifetime (several nanoseconds) was very small. Also, in the present study, a substantial difference in the average lifetime is observed for the two excitation wavelengths: It becomes much longer when relatively more outer antenna is excited at 465 nm as opposed to 400 nm. This means that a pool of LHCII is rather badly connected to the PSII cores (leading to long migration times and thus long fluorescence lifetimes) or

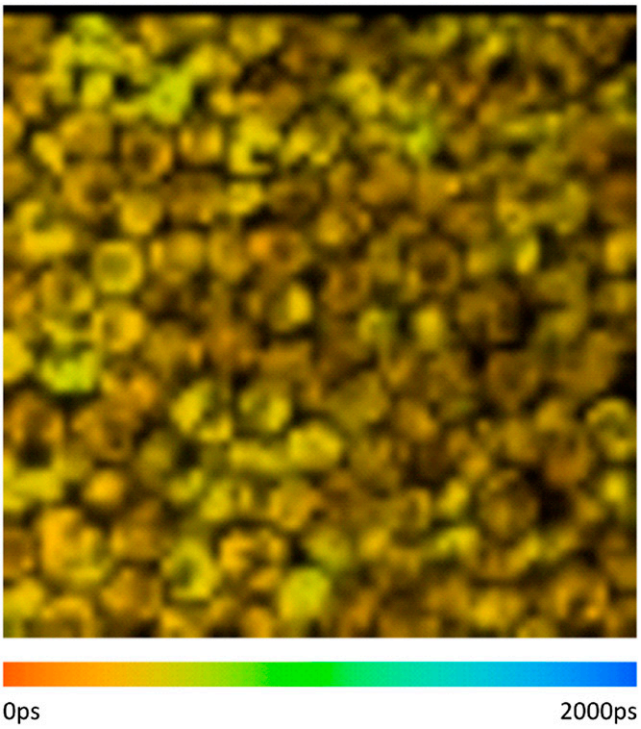

Fig. 3. Two-photon FLIM image of *C. reinhardtii* with the average lifetimes per pixel plotted using a color scale. The fluorescence decay in each pixel was analyzed by SPC image software, and the color scale is between 0 and 2,000 ps. (The average lifetime distribution is also given in a histogram in *SI Text*, Fig. S4.)

even completely disconnected, which from a functional point of view is nearly the same. Concurrently, this badly connected pool of LHCII is substantially quenched, considering the relatively short excited-state lifetimes. Remarkably, a large difference in excited-state lifetime for the two excitation wavelengths is observed both for states 1 and 2, meaning that in both states part of the antenna is disconnected from PSII. The existence of a pool of uncoupled LHCII in *C. reinhardtii* has been discussed in many studies on state transitions (28, 43). With the use of time-resolved fluorescence, we have now demonstrated that such an LHCII pool indeed exists, regardless of the state of the cell.

It is important to mention that the results obtained in the present study in fact agree with an early proposal by Allen and Melis (44), who, measuring cells of another green alga named *S. obliquus*, at that time claimed that during state transitions dissociated LHCII does not attach to PSI but instead is thermally deactivated, which means nothing else than that the fluorescence is quenched. Our results can also explain why Minagawa and coworkers (28) could follow the detachment of LHCII from PSII with the use of FLIM but did not report on what was happening after the detachment. Although it was reported in several studies that at least CP26, CP29, and LhcbM5 attach to PSI in state 2 (22–24, 43), our current data demonstrate that this can only be true for a relatively small fraction. As was stated above, even if only one LHCII trimer would move from PSII to PSI this would already lead to an increase of PSI amplitude by 6%, which is more than is experimentally observed. Therefore, it should be concluded that for the state 1-to-state 2 transition on average less than one LHCII trimer is moving from PSII to PSI. In fact, we have to conclude from our data that, even if LHCII detaches from PSII, only a fraction attaches to PSI, and in fact most of the detached antenna complexes aggregate, leading to a shortening of the excited-state lifetime. This shortening ensures that there is no increase in photodamage of the antenna complexes upon detachment, which would otherwise occur if quenching would be absent (45). The fact that only a small amount of antenna attaches to PSI in state 2 also explains why the amount of fluorescence of PSI at 77 K hardly increases (Fig. 1). In contrast, the PSII (and LHC) fluorescence drops substantially, in line with the observed decrease of the average lifetime at room temperature.

State Transitions: *Chlamydomonas reinhardtii* vs. *Arabidopsis thaliana*. Despite the fact that state transitions are present in plants and green algae, clear differences can be observed between this process in the model organisms *A. thaliana* and *C. reinhardtii.* In the plant *A. thaliana*, the amount of LHCII involved in the process is relatively small (around 10–15% of the population), and this mobile pool is part of the LHCII population that transfers energy relatively slowly to the PSII core in state 1 (6), but once it is attached to PSI (state 2) the transfer is extremely fast and efficient (6). The amount of LHCII that dissociates from PSII is identical to the amount that reassociates with PSI and serves to maintain a balance between PSI and PSII excitation. In the case of *C. reinhardtii*, we demonstrate here that state transitions seem to reduce the antenna size of PSII, whereas the effect on PSI is rather small; less than one LHCII trimer attaches per PSI complex on average. It has recently been demonstrated that, in the case of *A. thaliana*, the association of LHCII to PSI plays an important role in long-term acclimation to different intensities of growth light because the antenna size of both PSI and PSII can be modulated simply by the change in the amount of LHCII (Lhcb1 and Lhcb2), which in most conditions serve as antenna for both PSs (6). However, recent data on *C. reinhardtii* have underlined the important role of state transitions as a short-term response mechanism to increase photoprotection (46). This different role of state transitions in algae and plants seems to be related to the different mechanisms of nonphotochemical quenching (NPQ) in the two organisms. Whereas *A. thaliana* can switch on its photoprotective mechanism of NPQ within seconds in dangerous high-light conditions, due to the presence of the so-called PsbS protein in the membranes (47), this is not the case for *C. reinhardtii*, where the protein that is required for NPQ is expressed with a delay of several hours when the alga is put in high-light conditions (48). In this time period, photoprotection is assured by state transitions (46). Within this context, it makes sense that state transitions in *C. reinhardii* are mainly affecting the antenna size of PSII, which indeed needs to be immediately reduced in high-light conditions to avoid photodamage. A concomitant increase of the antenna size of PSI is not necessary, and it would even be detrimental, creating PSI damage (49). In this respect, there is again a resemblance with *A. thaliana*, where high-light stress is one of the very few conditions in which LHCII does not attach to PSI (6). Very interestingly, it has been found for *A. thaliana* that, in high light, as part of the NPQ mechanism, PsbS induces the detachment of a significant fraction of the outer antenna from PSII, which gets concomitantly quenched (50). This is very much reminiscent to what is now observed for *C. reinhardtii* during the process that has always been denoted as state transitions.

In conclusion, in contrast to what is generally believed, not 80% of the LHCII is moving from PSII to PSI upon the transition from state 1 to state 2 but only a small fraction (in the order of 10%). The rest of LHCII that detaches from PSII becomes quenched, and this detachment seems to play an important role in NPQ that protects PSII against dangerous overexcitation in high-light conditions, similar to what is happening in plants when PsbS is activated in high light.

Methods

Strains and Growth Conditions. WT *C. reinhardtii* (strain 137c) cells were grown under continuous white-light illumination in Tris-acetate-phophate medium (51). Cells were shaken in a rotary shaker (100 rpm) at 30 °C and illuminated by a white lamp at 10 $\mu mol \cdot m^2 \cdot s^{-1}$. All cells were grown in 250-mL flasks with a growing volume of 50 mL and maintained in the logarithmic growth phase. Also, a higher light intensity (100 $\mu mol \cdot m^2 \cdot s^{-1}$) was used to grow cells, and the results are shown in *SI Text* (Table S1).

State Locking. Cells were locked in state 1 or 2 in the following ways commonly used for state transitions studies on *C. reinhardtii* (21, 25, 32, 52, 53): State 1 was obtained by incubating the cells in the dark while vigorously shaking for 2 h (to oxidize the PQ pool with oxygen present), and state 2 was obtained by dark incubation in anaerobic conditions achieved by nitrogen bubbling for 25 min (to overreduce the PQ pool in the absence of oxygen) starting from cells in state 1, a method that was also applied by Delosme et al. (21, 32, 53). Cells were directly used for time-resolved fluorescence measurements without further treatment.

Fluorescence Measurements. ***Steady-state fluorescence.*** The 77 K steady-state fluorescence spectra were recorded with a Jobin Yvon Fluorolog FL3-22 spectrofluorimeter using liquid nitrogen and corrected for wavelength-dependent detection sensitivity and fluctuations in lamp output. The λ_{exc} was 440 nm; a bandwidth of 2 nm was used for excitation and emission. ***Time-resolved fluorescence.*** TCSPC measurements were performed with a home-built setup (54). Samples were excited with 400- and 465-nm pulses of 0.2 ps at repetition rate 3.8 MHz. To avoid closure of RCs and induction of unwanted state transitions, the excitation intensity was kept low (0.5–1.5 μW) with a count rate of 3,000 photons per second or lower. The size of the excitation spot was 2 mm. The IRF (40–50 ps FWHM) was obtained with pinacyanol iodide in methanol with 6-ps fluorescence lifetime (37, 42). Measurements were done for 5 min. Fluorescence was detected at 679, 701, and 720 nm using interference filters (15-nm width). Data were collected using a multichannel analyzer with a maximum time window of 4,096 channels at 5 or 2 ps per channel. One complete experiment consisted of recording datasets of reference compound, state-locked cells, and again reference compound, which was repeated at least twice with a fresh sample for each condition to check reproducibility.

Two-photon excitation (860 nm) FLIM was also performed in vivo; cells were pressed between microscope glass and cover glass, where they were kept for 10 min in darkness in order to precipitate/immobilize and adapt to the dark. The setup was described previously (37, 55). Fluorescence of *C. reinhardtii* was detected via nondescanned single-photon counting

detection, through two bandpass filters of 700 nm (75-nm width). The average lifetimes per pixel were analyzed with the SCP image software. All measurements were done at 22 °C.

Data analysis. Data obtained with the TCSPC setup were globally analyzed using the "TRFA Data Processing Package" of the Scientific Software Technologies Center (Belarusian State University, Minsk, Belarus). Fluorescence decay curves were fitted to multiexponential decay functions $(\sum_i p_i e^{-t/\tau_i})$ with relative amplitudes (p) and corresponding lifetimes (τ) that were convoluted with the IRF. The quality of a fit was judged from the χ^2 value and by visual inspection of residuals and autocorrelation thereof (Fig. S1). The number of exponentials was five in all cases, whereas one of these components was an artifact with lifetime between 0.1 and 1 ps, which was mainly used to improve the fit quality at early times. These artifacts are not further considered. The fit results were interpreted in terms of the average fluorescence lifetime (τ_{avg}) for τ_2, τ_3, and τ_4 according to $\tau_{avg} = \sum_{i=2}^{4} p_i \tau_i$ where $\sum_{i=1}^{4} p_i = 1$.

ACKNOWLEDGMENTS. This work was supported financially by the Netherlands Organization for Scientific Research via the Council for Chemical Sciences (H.v.A.) and by European Research Council (ERC) Consolidator Grant 281341 (to R.C.).

1. Jordan P, et al. (2001) Three-dimensional structure of cyanobacterial photosystem I at 2.5 A resolution. *Nature* 411(6840):909–917.
2. Liu ZF, et al. (2004) Crystal structure of spinach major light-harvesting complex at 2.72 A resolution. *Nature* 428(6980):287–292.
3. Croce R, van Amerongen H (2011) Light-harvesting and structural organization of photosystem II: From individual complexes to thylakoid membrane. *J Photochem Photobiol B* 104(1-2):142–153.
4. Wientjes E, van Amerongen H, Croce R (2013) Quantum yield of charge separation in photosystem II: Functional effect of changes in the antenna size upon light acclimation. *J Phys Chem B* 117(38):11200–11208.
5. Ben-Shem A, Frolow F, Nelson N (2003) Crystal structure of plant photosystem I. *Nature* 426(6967):630–635.
6. Wientjes E, van Amerongen H, Croce R (2013) LHCII is an antenna of both photosystems after long-term acclimation. *Biochim Biophys Acta* 1827(3):420–426.
7. Drop B, et al. (2011) Photosystem I of *Chlamydomonas reinhardtii* contains nine light-harvesting complexes (Lhca) located on one side of the core. *J Biol Chem* 286(52): 44878–44887.
8. Elrad D, Grossman AR (2004) A genome's-eye view of the light-harvesting polypeptides of *Chlamydomonas reinhardtii*. *Curr Genet* 45(2):61–75.
9. Tokutsu R, Kato N, Bui KH, Ishikawa T, Minagawa J (2012) Revisiting the supramolecular organization of photosystem II in *Chlamydomonas reinhardtii*. *J Biol Chem* 287(37):31574–31581.
10. Drop B, et al. (2014) Light-harvesting complex II (LHCII) and its supramolecular organization in *Chlamydomonas reinhardtii*. *Biochimica Et Biophysica Acta-Bioenergetics* 1837(1):63–72.
11. Murata N (1969) Control of excitation transfer in photosynthesis. I. Light-induced change of chlorophyll a fluorescence in *Porphyridium cruentum*. *Biochim Biophys Acta* 172(2):242–251.
12. Bonaventura C, Myers J (1969) Fluorescence and oxygen evolution from *Chlorella pyrenoidosa*. *Biochim Biophys Acta* 189(3):366–383.
13. Allen JF, Bennett J, Steinback KE, Arntzen CJ (1981) Chloroplast protein-phosphorylation couples plastoquinone redox state to distribution of excitation-energy between photosystems. *Nature* 291(5810):25–29.
14. Allen JF (1992) Protein phosphorylation in regulation of photosynthesis. *Biochim Biophys Acta* 1098(3):275–335.
15. Kouril R, et al. (2005) Structural characterization of a complex of photosystem I and light-harvesting complex II of *Arabidopsis thaliana*. *Biochemistry* 44(33):10935–10940.
16. Bellafiore S, Barneche F, Peltier G, Rochaix JD (2005) State transitions and light adaptation require chloroplast thylakoid protein kinase STN7. *Nature* 433(7028):892–895.
17. Depège N, Bellafiore S, Rochaix JD (2003) Role of chloroplast protein kinase Stt7 in LHCII phosphorylation and state transition in *Chlamydomonas*. *Science* 299(5612):1572–1575.
18. Bonardi V, et al. (2005) Photosystem II core phosphorylation and photosynthetic acclimation require two different protein kinases. *Nature* 437(7062):1179–1182.
19. Shapiguzov A, et al. (2010) The PPH1 phosphatase is specifically involved in LHCII dephosphorylation and state transitions in *Arabidopsis*. *Proc Natl Acad Sci USA* 107(10):4782–4787.
20. Wijffels RH, Barbosa MJ (2010) An outlook on microalgal biofuels. *Science* 329(5993): 796–799.
21. Delosme R, Olive J, Wollman FA (1996) Changes in light energy distribution upon state transitions: An in vivo photoacoustic study of the wild type and photosynthesis mutants from *Chlamydomonas reinhardtii*. *Biochim Biophys Acta* 1273(2):150–158.
22. Iwai M, Takahashi Y, Minagawa J (2008) Molecular remodeling of photosystem II during state transitions in *Chlamydomonas reinhardtii*. *Plant Cell* 20(8):2177–2189.
23. Takahashi H, Iwai M, Takahashi Y, Minagawa J (2006) Identification of the mobile light-harvesting complex II polypeptides for state transitions in *Chlamydomonas reinhardtii*. *Proc Natl Acad Sci USA* 103(2):477–482.
24. Tokutsu R, Iwai M, Minagawa J (2009) CP29, a monomeric light-harvesting complex II protein, is essential for state transitions in *Chlamydomonas reinhardtii*. *J Biol Chem* 284(12):7777–7782.
25. Kargul J, et al. (2005) Light-harvesting complex II protein CP29 binds to photosystem I of *Chlamydomonas reinhardtii* under State 2 conditions. *FEBS J* 272(18):4797–4806.
26. Hodges M, Mova I (1987) Time-resolved chlorophyll fluorescence studies on photosynthetic mutants of *Chlamydomonas reinhardtii*: Origin of the kinetic decay components. *Photosynth Res* 13(2):125–141.
27. Wendler J, Holzwarth AR (1987) State transitions in the green alga scenedesmus obliquus probed by time-resolved chlorophyll fluorescence spectroscopy and global data analysis. *Biophys J* 52(5):717–728.
28. Iwai M, Yokono M, Inada N, Minagawa J (2010) Live-cell imaging of photosystem II antenna dissociation during state transitions. *Proc Natl Acad Sci USA* 107(5):2337–2342.
29. Amarnath K, Zaks J, Park SD, Niyogi KK, Fleming GR (2012) Fluorescence lifetime snapshots reveal two rapidly reversible mechanisms of photoprotection in live cells of *Chlamydomonas reinhardtii*. *Proc Natl Acad Sci USA* 109(22):8405–8410.
30. van Oort B, et al. (2010) Effect of antenna-depletion in Photosystem II on excitation energy transfer in *Arabidopsis thaliana*. *Biophys J* 98(5):922–931.
31. Holzwarth AR, Lenk D, Jahns P (2013) On the analysis of non-photochemical chlorophyll fluorescence quenching curves: I. Theoretical considerations. *Biochim Biophys Acta* 1827(6):786–792.
32. Fleischmann MM, et al. (1999) Isolation and characterization of photoautotrophic mutants of *Chlamydomonas reinhardtii* deficient in state transition. *J Biol Chem* 274(43):30987–30994.
33. Broess K, et al. (2006) Excitation energy transfer and charge separation in photosystem II membranes revisited. *Biophys J* 91(10):3776–3786.
34. Broess K, Trinkunas G, van Hoek A, Croce R, van Amerongen H (2008) Determination of the excitation migration time in Photosystem II consequences for the membrane organization and charge separation parameters. *Biochim Biophys Acta* 1777(5):404–409.
35. Barzda V, et al. (2001) Fluorescence lifetime heterogeneity in aggregates of LHCII revealed by time-resolved microscopy. *Biophys J* 81(1):538–546.
36. Krumova SB, et al. (2010) Monitoring photosynthesis in individual cells of *Synechocystis* sp. PCC 6803 on a picosecond timescale. *Biophys J* 99(6):2006–2015.
37. van Oort B, et al. (2008) Picosecond fluorescence of intact and dissolved PSI-LHCI crystals. *Biophys J* 95(12):5851–5861.
38. Bennett J, Steinback KE, Arntzen CJ (1980) Chloroplast phosphoproteins: Regulation of excitation energy transfer by phosphorylation of thylakoid membrane polypeptides. *Proc Natl Acad Sci USA* 77(9):5253–5257.
39. Pribil M, Pesaresi P, Hertle A, Barbato R, Leister D (2010) Role of plastid protein phosphatase TAP38 in LHCII dephosphorylation and thylakoid electron flow. *PLoS Biol* 8(1):e1000288.
40. Tikkanen M, Grieco M, Kangasjärvi S, Aro EM (2010) Thylakoid protein phosphorylation in higher plant chloroplasts optimizes electron transfer under fluctuating light. *Plant Physiol* 152(2):723–735.
41. Tikkanen M, et al. (2006) State transitions revisited-a buffering system for dynamic low light acclimation of *Arabidopsis*. *Plant Mol Biol* 62(4-5):779–793.
42. van Oort B, van Hoek A, Ruban AV, van Amerongen H (2007) Aggregation of light-harvesting complex II leads to formation of efficient excitation energy traps in monomeric and trimeric complexes. *FEBS Lett* 581(18):3528–3532.
43. Minagawa J (2011) State transitions—the molecular remodeling of photosynthetic supercomplexes that controls energy flow in the chloroplast. *Biochim Biophys Acta* 1807(8):897–905.
44. Allen JF, Melis A (1988) The rate of P-700 photooxidation under continuous illumination is independent of state-1 state-2 transitions in the green-alga *Scenedesmus obliquus*. *Biochim Biophys Acta* 933(1):95–106.
45. Ruban AV, et al. (2007) Identification of a mechanism of photoprotective energy dissipation in higher plants. *Nature* 450(7169):575–578.
46. Allorent G, et al. (2013) A dual strategy to cope with high light in *Chlamydomonas reinhardtii*. *Plant Cell* 25(2):545–557.
47. Li XP, et al. (2000) A pigment-binding protein essential for regulation of photosynthetic light harvesting. *Nature* 403(6768):391–395.
48. Peers G, et al. (2009) An ancient light-harvesting protein is critical for the regulation of algal photosynthesis. *Nature* 462(7272):518–521.
49. Grieco M, Tikkanen M, Paakkarinen V, Kangasjärvi S, Aro E-M (2012) Steady-state phosphorylation of light-harvesting complex II proteins preserves photosystem I under fluctuating white light. *Plant Physiol* 160(4):1896–1910.
50. Holzwarth AR, Miloslavina Y, Nilkens M, Jahns P (2009) Identification of two quenching sites active in the regulation of photosynthetic light-harvesting studied by time-resolved fluorescence. *Chem Phys Lett* 483(4-6):262–267.
51. Gorman DS, Levine RP (1965) Cytochrome f and plastocyanin: Their sequence in the photosynthetic electron transport chain of *Chlamydomonas reinhardi*. *Proc Natl Acad Sci USA* 54(6):1665–1669.
52. Wollman FA, Delepelaire P (1984) Correlation between changes in light energy distribution and changes in thylakoid membrane polypeptide phosphorylation in *Chlamydomonas reinhardtii*. *J Cell Biol* 98(1):1–7.
53. Finazzi G, Barbagallo RP, Bergo E, Barbato R, Forti G (2001) Photoinhibition of *Chlamydomonas reinhardtii* in State 1 and State 2: Damages to the photosynthetic apparatus under linear and cyclic electron flow. *J Biol Chem* 276(25):22251–22257.
54. Somsen OJG, Keukens LB, de Keijzer MN, van Hoek A, van Amerongen H (2005) Structural heterogeneity in DNA: Temperature dependence of 2-aminopurine fluorescence in dinucleotides. *ChemPhysChem* 6(8):1622–1627.
55. Russinova E, et al. (2004) Heterodimerization and endocytosis of *Arabidopsis* brassinosteroid receptors BRI1 and AtSERK3 (BAK1). *Plant Cell* 16(12):3216–3229.